Journal of Physics: Conference Series

A preliminary study of phases, elemental mapping, and electrical properties on Na_2FeSiO_4 derived from rice husk silica

Journal of Physics: Conference Series **1572** (2020) 012003 doi:10.1088/1742-6596/1572/1/012003

A preliminary study of phases, elemental mapping, and electrical properties on Na_2FeSiO_4 derived from rice husk silica

A Riyanto*, S Sembiring, A R Amalia, A Astika and R Marjunus

Department of Physics, University of Lampung, Bandarlampung, Indonesia

*E-mail: agus.riyanto@fmipa.unila.ac.id

Abstract. This work reports a preliminary investigation about the phase, element mapping, and electrical properties of Na_2FeSiO_4 prepared from rice husk silica, $(FeNO_3)_3.9H_2O$, NaOH, and $C_6H_8O_7.H_2O$ using the sol-gel method. A sample sintered at 800 °C with a holding time of 10 hours at peak temperature. The phases identification shows that the main phase of Na_2FeSiO_4 had been formed in the sample accompanied by two impurity phases, i.e., Na_2SiO_3 and SiO_2. Elemental mapping shows that Na, Fe, Si, and O elements are evenly distributed over the entire surface of the sample. The band gap energy value of the sample is relatively small, around 2.58 eV - 2.87 eV. Its electrical conductivity varies depending on frequency, i.e., $6.13x10^{-5}$ S/m at 1 Hz and decreases gradually up to $4.27x10^{-5}$ S/m at 1000 Hz.

1. Introduction

The search for new cathode materials has become a severe concern for researchers to create batteries with high specific capacities and low production costs. Li_2FeSiO_4 orthosilicate with polyanion structure attracts the interest of researchers because the structure of the material allows the presence of two lithium ions per formula. Because of that, it can produce high specific capacities; theoretically, it can reach 330 $mAhg^{-1}$ [1-2]. The material also has lattice stability compared to other polyanion materials but shows poor electrical conductivity [3]. Besides, the limited availability of lithium causes the cost of making Li_2FeSiO_4 to be expensive [4]. Therefore, other materials with similar characteristics but abundant raw materials available in nature need to be developed. Na_2FeSiO_4 is a new type of polyanion material that can be used as an alternative to Li_2FeSiO_4 because it has a similar ionic radius and potential redox characteristics [5-8]. Na_2FeSiO_4 has excellent structural stability similar to Li_2FeSiO_4, and high theoretical specific capacity reaches 278 $mAhg^{-1}$ [9–11]. Although, in theory, Na_2FeSiO_4 has a slightly lower specific capacity than Li_2FeSiO_4, Na_2FeSiO_4 has much higher electrical conductivity and cheaper and also abundant raw materials compared to Li_2FeSiO_4. Electrical conductivity is one crucial factor in determining the performance of a cathode [12]. Therefore, Na_2FeSiO_4 is very potential to be developed as a cathode material.

Na_2FeSiO_4 can be produced using various types of methods, a kind of simple technique that is widely applied is the sol-gel method [13-14]. The source of silica used in this production is generally derived from tetraethyl orthosilicate (TEOS) [14-17]. The use of TEOS as a source of silica may be replaced with silica from rice husk to reduce production costs [18-19]. Rice husk has abundant availability in nature, and from that, rice husk can be extracted with silica reaching 99% purity through simple methods [20]. Besides, silica from rice husk has an amorphous structure and reactive so that it

can be used as a raw material in the manufacture of various materials [21-22]. In our previous studies, rice husk silica was successfully used as a raw material for forsterite [23-24] and cordierite [25-26]. By utilizing rice husk silica in the process of making various materials, especially Na_2FeSiO_4, it can reduce production costs.

In this work, we prepare Na_2FeSiO_4 derived from rice husk silica. Preparation was carried out using the sol-gel method and followed by thermal treatment at 800 °C. The work aims to investigate the potential of rice husk silica as a raw material in the manufacture of Na_2FeSiO_4 and investigate the possibility of Na_2FeSiO_4 as a cathode in batteries system considered from its electrical characteristics. This work clearly describes the structure and electrical properties of the Na_2FeSiO_4 sample, which included functional groups, phases, morphology, elemental distribution, bandgap energy, and electrical conductivity.

2. Materials and methods

2.1. Silica extraction from rice husk

Silica was extracted from rice husk refers to our previous study [27]. As much as 50 grams of rice husk was boiled in 500 ml of 5% KOH solution. The mixture obtained from this process was then left in room temperature for 24 hours and then filtered to obtain a silica sol. Silica sol was added 10% HNO_3 solution by dropwise to form a gel with a pH of 7. The gel was cleaned using deionized water and then dried at 110 °C to obtain a solid. The solid was ground and then sieve to get silica powder with particle size 200 meshes.

2.2. Na_2FeSiO_4 preparation

Na_2FeSiO_4 preparation using the sol-gel method refers to previously reported studies [28-31]. Na_2FeSiO_4 was prepared from $(FeNO_3)_3.9H_2O$, NaOH, rice husk silica, and $C_6H_8O_7.H_2O$ with a mole ratio of 1:2:1:1. Silica powder was dissolved in NaOH at 60 °C for 30 minutes, then added $(FeNO_3)_3.9H_2O$ and $C_6H_8O_7.H_2O$ solution by dropwise until it reached pH 1. The mixture was refluxed at 80 °C for 5 hours and then poured to the beaker glass. It was evaporated at 75 °C under magnetic stirring until a gel was obtained. The gel was dried at 130 °C for 3 hours and then ground to get a fine powder. After that, the fine powder was sintered at 800 °C with a temperature of 3 °C/minute and a holding time of 10 hours at peak temperature.

2.3. Functional groups analysis

Na_2FeSiO_4 sample and KBr powder were ground and then pressed into a pellet. The functional groups in the prepared pellet were analyzed using the Nicolet iS10 FTIR Spectrometer by scanning in the wavelength range of 1250-400 cm^{-1}. The analysis was conducted by comparing the FTIR spectrum with references published in previous studies.

2.4. Phase analysis

The phases were characterized by X'Pert Powder PW 30/40 XRD with Cu-Kα radiation. Samples were scanned at 2θ 10°-100°. Phase analysis was carried out using the search match method using Qual X software version 2.24 with Crystallography Open Database (COD).

2.5. Surface morphology and elemental distribution analysis

The surface morphology and distribution of the elements in the samples were analyzed using SEM/EDS Tescan Vega3.

2.6. Band gap energy estimation

Shimadzu UV-2450 UV-Vis spectrophotometer was used to measure the diffuse reflection of Na_2FeSiO_4 sample powder in the wavelength range of 200-800 nm. The band gap energy was estimated using the Kubelka-Munk theorem shown by Equation (1)

$$F(R) = K/S = (1-R)^2/2R \quad (1)$$

where $F(R)$ is the function of Kubelka-Munk, S and K are the scattering and absorption coefficients respectively, and R is the diffuse reflection. The band gap (E_g) and the absorption coefficient is related through the Tauc relation. Tauc relation to the direct band gap is given in Equation (2)

$$(\alpha h\nu) = A\left(h\nu - E_g\right)^{1/2} \quad (2)$$

where α is the linear absorption coefficient, $h\nu$ is photon energy, A is the proportional constant, and E_g is band gap. When incident radiation scatters are perfectly diffuse manner, the absorption coefficient K becomes equal to 2α. In this case, considering the scattering coefficient S as constant concerning wavelength, the Kubelka-Munk is proportional to the absorption coefficient α, applying Equation 1 can be obtained from the relation such as Equation (3)

$$[F(R)h\nu]^2 = A\left(h\nu - E_g\right) \quad (3)$$

2.7. Electrical conductivity measurement

LCR meter was used to measure the conductance of Na_2FeSiO_4 pellet with a diameter of $1x10^{-2}$ m and a thickness of $3x10^{-3}$ m. The conductance was measured in the frequency range of 1-1000 Hz. The value of the conductance was converted to electrical conductivity using Equation (4)

$$\sigma = G\ l/A \quad (4)$$

where σ is the electrical conductivity (S/m), G is the conductance (S), l and A are thickness (m) and cross-section of the sample (m^2), respectively.

3. Result and discussion

The FTIR spectrum of the Na_2FeSiO_4 sample shown in Figure 1. It shows the presence of several absorption peaks associated with a typical functional group contained in the Na_2FeSiO_4 compound. The absorption peaks at wave numbers 972.12 cm^{-1} and 879.54 cm^{-1} are related to the vibration stretching of the Si-O group from SiO_4 tetrahedra [32]. Absorption peaks at wave numbers 640.37 cm^{-1} and 509.21 cm^{-1} are related to the vibration stretching of the Fe-O group of [FeO_4] tetrahedra [33]. Meanwhile, the absorption peak at wave number 432.05 cm^{-1} indicates the presence of vibration of the Na-O group of [NaO_4] tetrahedra [34]. The appearance of the absorption peaks of the Si-O, Fe-O, and Na-O groups in the FTIR spectrum shows a strong indication that the Na_2FeSiO_4 phase has formed in the sample.

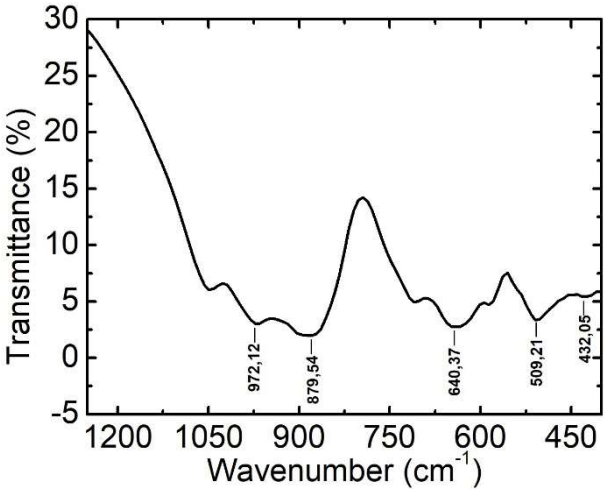

Figure 1. FTIR spectrum of a sample of Na_2FeSiO_4 derived from rice husk silica.

The diffractogram of the Na_2FeSiO_4 sample shown in Figure 2. The phase analysis conducted by comparing the diffraction lines with the COD database using the search-match method. Referring to previous studies [17], because Na_2FeSiO_4 is not yet available in the database, the analysis may use crystallographic databases of similar polyanion compounds, for example, Na_2CaSiO_4. The compounds have the same crystal structure. The characterization showed that the diffraction line from the Na_2FeSiO_4 sample was in agreement with the database of Na_2CaSiO_4 (COD 00-101-0111) which was marked by the presence of diffraction peaks at 2θ of 16.82°; 20.47°; 29.36°; 33.72°; 48.47°; 60.38°; and 81.09° which correspond to the Miller index (110), (111), (211), (220, (412), (400), (422) and (602) respectively. According to studies conducted by Kee et al., (2016), the formation of the Na_2FeSiO_4 phase was characterized by the presence of diffraction peaks with the Miller index [17]. The presence of a diffraction peak at 2θ of 33.72 °, which is the peak with the highest intensity, confirms that the phase is the main phase in the sample. The establishment of this phase is in agreement with the results of FTIR analysis, which shows the presence typically functional groups of the Na_2FeSiO_4 structure, such as Na-O, Fe-O, and Si-O [35]. Besides the crystalline phase Na_2FeSiO_4, the diffractogram also shows diffraction peaks, which indicate the presence of impurity phases such as Na_2SiO_3 (COD 00-231-08580) and SiO_2 (COD 00-900-0520) as shown in Figure 2. The presence of the Na_2SiO_3 phase is characterized by the appearance of the diffraction peak at 2θ of 29.65°, which is the main peak of the phase as well as several other diffraction peaks, as shown in Figure 2. Whereas, the presence of the SiO_2 phase is characterized by the appearance of the peak diffraction peak at 2θ of 20.50°. The formation of this impurity phase is predicted as a result of thermal energy given to the sample in the thermal treatment that does not sufficiently encourage the entire crystallization process to form the Na_2FeSiO_4 phase.

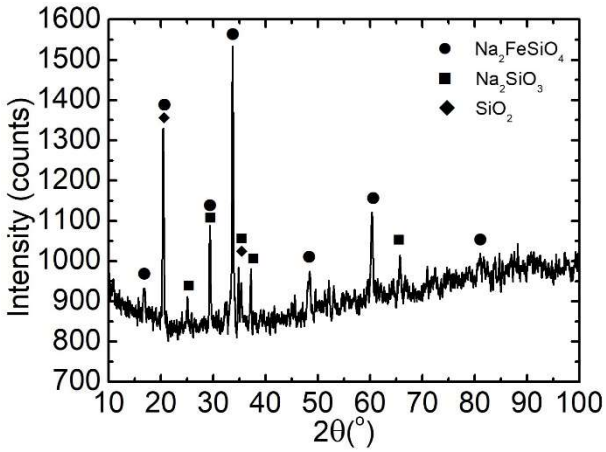

Figure 2. Diffractogram of a sample of Na_2FeSiO_4 derived from rice husk silica.

SEM analysis shows that the Na_2FeSiO_4 sample is consists of micro-scale particles, as shown in Figure 3(a). The constituent elements of Na_2FeSiO_4, i.e., sodium (Na), iron (Fe), silicon (Si), and oxygen (O), appear to be evenly distributed on the sample surface as shown in Figure 3(b). The distribution of the elements sodium (Na), silicon (Si) and oxygen (O) on the surface are clearly shown in Figure 3(c)-(f). This mapping element reinforces the results of the phase analysis, which identifies the formation of the Na_2FeSiO_4 phase, as well as the impurity phase. The results also confirm that silica from the husk is very potential to be used as a raw material in the synthesis of Na_2FeSiO_4.

The band gap energy value of the Na_2FeSiO_4 sample is estimated using the Tauc plot, as shown in Figure 4(a). The Tauc plot has two dominant slopes that intersect the x-axis at 2.58 eV and 2.87 eV. It means that the sample has two different band gaps, i.e., 2.58 eV and 2.87 eV. The presence of two band gap values in the sample is due to the presence of the impurity phase in the sample [36]. This situation is consistent with the results of the phase analysis, which shows the presence of the impurity phases. The band gap energy value estimated from the Tauc plot is low. A high electrical conductivity value follows the low band gap energy value. The electrical conductivity value in frequencies 1-1000 Hz and shown in Figure 4(b). The electrical conductivity of the sample varies with frequency, at a frequency of 1 Hz is 6.13×10^{-5} S/m, and then decreases gradually to 4.27×10^{-5} S/m at a frequency of 1000 Hz. In general, the electrical conductivity of the Na_2FeSiO_4 sample along the measurement frequency has a much higher value than Na_2FeSiO_4, which is only in the order of $\sim 10^{-12}$ S/m [37]. By considering the characteristics of the electrical properties obtained, it shows that the Na_2FeSiO_4 samples prepared from rice husk silica have a high potential for use as a cathode.

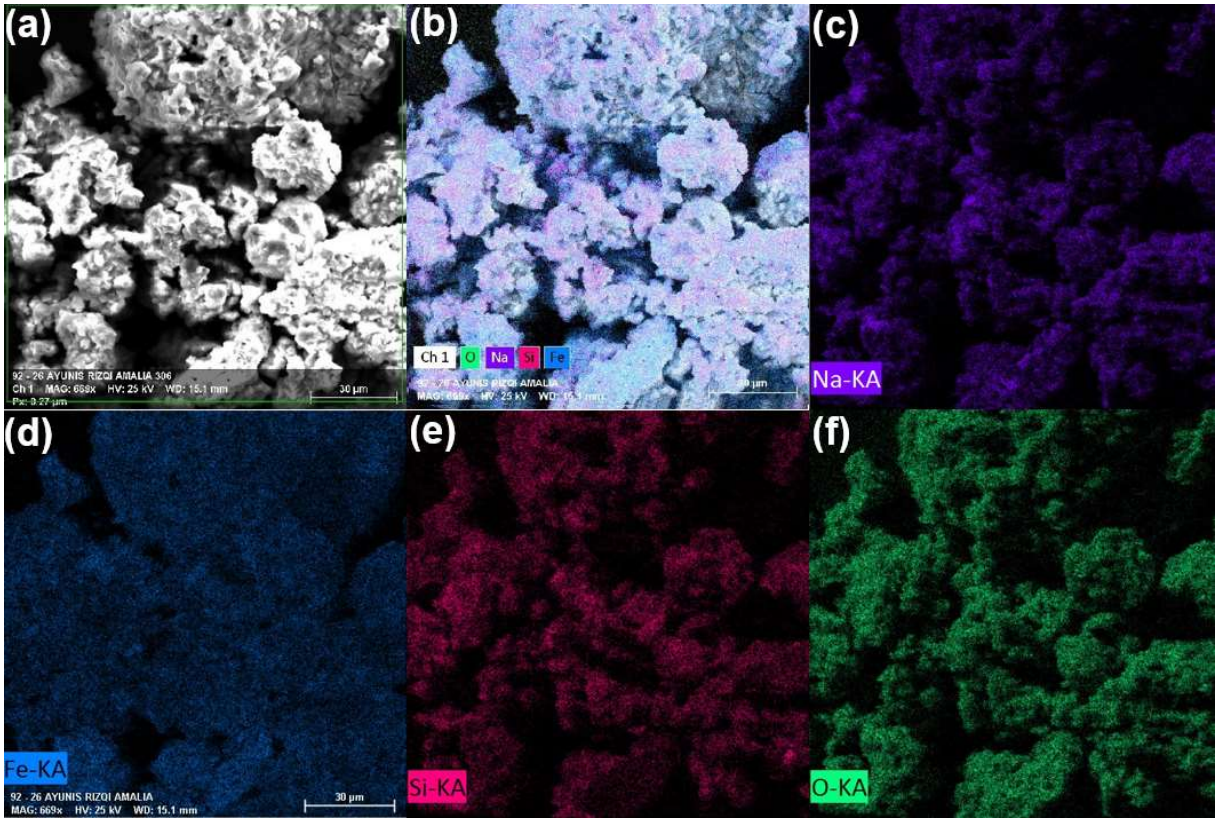

Figure 3. (a) Morphology and elements mapping in a sample of Na_2FeSiO_4 derived from rice husk silica, (b) element distribution, (c) Na, (d) Fe, (e) Si, and (f) O distribution.

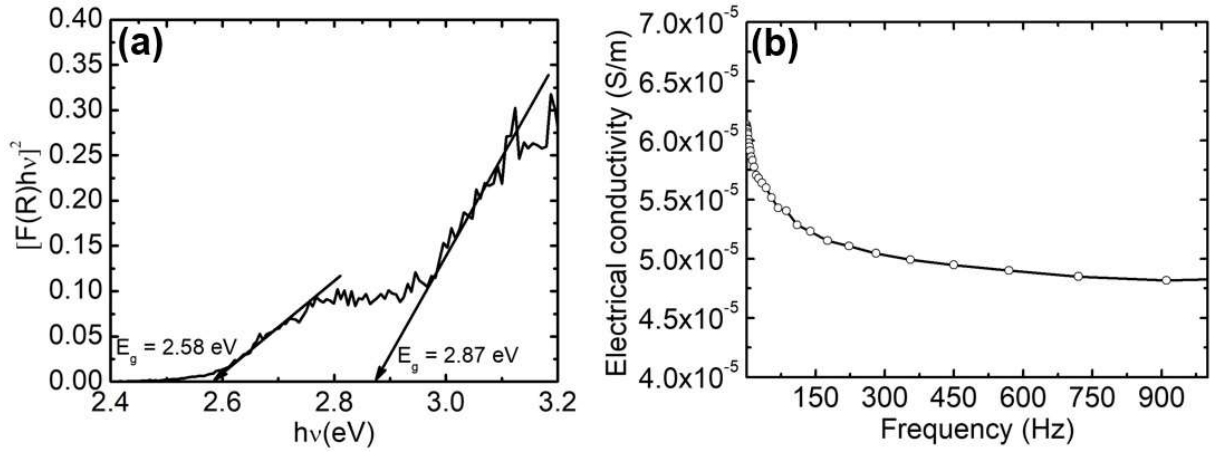

Figure 4. (a) Tauc plot of band gap energy, and (b) Electrical conductivity of a sample of Na_2FeSiO_4.

4. Conclusions

Silica from rice husk is very potential to be used as a raw material in the production of Na_2FeSiO_4, although phase analysis shows the presence of impurities that accompany the primary phase. The formation of the Na_2FeSiO_4 phase is supported by the FTIR analysis, which indicates the presence of functional groups that are typical of Na_2FeSiO_4, i.e., Na-O, Fe-O, and Si-O groups from the tetrahedra side. The mapping of the elements also strengthens the formation of this phase. The mapping elements

show that Na, Fe, Si, and O homogeneously distributed on the surface of the sample. Tauc plot indicates that the Na_2FeSiO_4 has a band gap value of around 2.58-2.87 eV and electrical conductivity $6.13x10^{-5}$ S/m at 1 Hz and decreases gradually up to $4.27x10^{-5}$ S/m at 1000 Hz. This value is far higher than the electrical conductivity of Li_2FeSiO_4. From the electrical conductivity, Na_2FeSiO_4 prepared from rice husk silica has excellent potential for use as a cathode material.

5. References

[1] Gong Z and Yang Y. 2011. Recent advances in the research of polyanion-type cathode materials for Li-ion batteries. *Energy Environ. Sci.* **4**: 3223–42

[2] Bianchini F, Fjellvag H and Vajeeston P. 2017. First-principles study of the structural stability and electrochemical properties of Na_2MSiO_4 (M = Mn, Fe, Co and Ni) polymorphs. *Phys. Chem. Chem. Phys.* **19**: 14462-470

[3] Zhang S, Deng C, Fu B. L, Yang S and Ma L. 2010. Doping effects of magnesium on the electrochemical performance of Li_2FeSiO_4 for lithium ion batteries. *J. Electroanal. Chem.* **644**: 150-4

[4] Jian Z, Yu H and Zhou H. 2013. Designing high-capacity cathode materials for sodium-ion batteries. *Electrochem. Commun.* **34**: 215-18

[5] Yabuuchi N, Kubota K, Dahbi M and Komaba S. 2014. Research development on sodium-ion batteries. *Chem. Rev.* **114**: 11636−82

[6] Palomares V, Serras P, Villaluenga I, Hueso K B and Gonzales J C. 2012. Na-ion batteries, recent advances and present challenges to become low cost energy storage system. *Energy Environ. Sci.* **5***:* 5884-901

[7] Hwang J Y, Myung S T and Sun Y K. 2017. Sodium-ion batteries: Present and future. *Chem. Soc. Rev.* **46**(12): 3485-856

[8] Nayak P K, Yang L, Brehm W and Adelhelm P. 2018. From lithium-ion to sodium-ion batteries: Advantages. *Angew. Chem.* **57**: 102-120

[9] Feng Z, Tang M and Yan Z. 2018. 3D conductive CNTs anchored with Na_2FeSiO_4 nanocrystals as a novel cathode material for electrochemical sodium storage. *Ceram. Int.* **44**(17): 22019-22

[10] Ye Z, Li S, Wu S, Wu P, Nguyen M C, Guo J, Mi J, Gong Z, Zhu Z Z, Yang Y, Wang Z C and Ho K M. 2016. Robust diamond-like Fe-Si network in the zero-strain Na_xFeSiO_4. *Electrochim. Acta* **212**: 934-40

[11] Guo S P, Li J C, Xu Q T, Ma Z and Xue H G. 2017. Recent achievements on polyanion-type compounds for sodium-ion. *J. Power Sources* **361**: 285-99

[12] Li Y, Sun W, Liang J, Sun H, Marco I, Ni L, Tang S and Zhang J. 2016. Understanding the electrochemical properties of A_2MSiO_4 (A = Li and Na; M = Fe, Mn, Co and Ni) and the Na doping effect on Li_2MSiO_4 from first principle calculation. *J. Mater. Chem.* **4**(44): 17455-63

[13] Li S, Guo J, Ye Z, Zhao X, Wu S, Mi J X,Yang Y, Wang C and Ho K. 2016. A zero-strain Na_2FeSiO_4 as novel cathode material sodium ion batteries. *ACS Appl. Mater. Intefaces* **8**(27): 17233-38

[14] Guan W, Pan B, Zhou P, Mi J, Zhang D, Xu J and Jiang Y. 2017. A high capacity, good safety and low cost Na_2FeSiO_4-Based cathode for rechargeable sodium-ion battery. *ACS Appl. Mater. Intefaces* **9**(27): 22369–77

[15] Feng Z, Tang M and Yan Z. 2018. 3D conductive CNTs anchored with Na_2FeSiO_4 nanocrystals as a novel cathode material for electrochemical sodium storage. *Ceram. Int.* **44**(17): 22019-22

[16] Kaliyappan K and Chen Z. 2018. Facile solid-state synthesis of eco-friendly sodium iron silicate with exceptional sodium storage behavior. *Electrochim. Acta* **283**: 1384-89

[17] Kee Y, Dimov N, Staykov A and Okada S. 2016. Investigation of metastable Na_2FeSiO_4 as a cathode material for Na-ion. *Mater. Chem. Phys.* **171**: 45-49

[18] Prasad R and pandey M. 2012. Rice husk ash as renewable source for the production of value added silica gel and its application; An overview. *Bull. Chem. React. Eng. Catal.* **7**(1): 1-25
[19] Todkar B S, Deorukhkar O A and Deshmukh S M. 2016. Extraction of silica from rice husk. *Int. J. Eng. Res. Dev.* **12**(3): 60-74
[20] Johan E, Ogami k, Matsue N, Itagaki Y and Aono H. 2016. Fabrication of high purity silica from rice husk and its conversion into ZSM-5. *ARPN J. Eng. Appl. Sci.* **11**(6): 4006-10
[21] Bakar R A, Yahya R and Gan S N. 2016. *Production of high purity amorphous silica from rice husk*. 5th International Conference on Recent Advances in Materials, Minerals and Environment (RAMM) and 2nd International Postgraduate Conference on Materials, Mineral and Polymer (MAMIP). Malaysia: Elsevier **19**: 189-95
[22] Rivas A L, Vera G, Palacios V, Cornejo M, Rigail A and Solórzano G. 2018. *Phase Transformation of Amorphous Rice Husk Silica*. Frontiers in Materials Processing, Applications, Research and Technology. Singapore: Springer Nature Singapure Pte Ltd: 17-27
[23] Sembiring S, Riyanto A, Simanjuntak W and Situmeang R. 2017. Effect of MgO-SiO_2 ratio on the forsterite (Mg_2SiO_4) precursors characteristics derived from amorphous rice husk silica. *Orient. J. Chem.* **33**(4): 1828-36
[24] Sembiring S, Riyanto A, Rumiyanti L, Sembiring Z and Situmeang R. 2019. Effect of sintering temperature on the structural and physical properties of forsterite using amorphous rice husk silica as refractory precursors. *J. Aust. Ceram. Soc.* **3**(8): 1-8
[25] Sembiring S, Simanjuntak W, Situmeang R, Riyanto A and Sebayang K. 2016. Preparation of refractory cordierite using amorphous rice husk silica for thermal insulation purposes. *Ceram. Int.* **42**: 8431-7
[26] Sembiring S, Simanjuntak W, Situmeang R, Riyanto A and Junaidi. 2018. Structural and physical properties of refractory cordierite precursors prepared from rice husk silica with different MgO addition. Ceramics-Silikåty **62**(2): 163-72
[27] Sembiring S, Simanjuntak W, Situmeang R, Riyanto A and Karo-Karo P. 2017. Effect of alumina addition on the phase transformation and crystallisation properties of refractory coerdierite prepared from amorphous rice husk silica. *J. Asian Ceram. Soc.* **5**(2): 186-92
[28] Zhang S, Deng C and Yang S. 2009. Preparation of nano-Li_2FeSiO_4 as cathode material for lithium-ion batteries. *Electrochem. Solid-State Lett.* **63**(2): A136-9
[29] Meenakshi V, Rajkumar P, Diwakar K, Subadevi R and Sivakumar M. 2016. *Structural investigation of heat-treated Li_2FeSiO_4 cathode material preparation*. International seminar on Nanoscience and Technology **3**: 10-2
[30] Crundwell F. 2014. The mechanism of dissolution of minerals in acidic and alkaline solutions: Part II Application of a new theory to silicates, aluminosilicates and quartz. *Hydrometallurgy* **149**: 265-75
[31] Zhou H, Einarsrud M A and Vullum-Breur F. 2013. High capacity nanostructured $Li_2Fe_xSiO_4$/C with Fe hyperstoichiometry for Li-ion batteries. *J. Power Source* **235**: 234-42
[32] Ghaffari A and Behzad M. 2018. Facile synthesis of layered sodium disilicates as efficient and recoverable nanocatalysts for biodiesel production from rapeseed oil. *Adv. Powder Technol.* **29**(5): 1265-71
[33] Jain R, Luthra V, Aurora M and Gokhale S. 2018. Infrared spectroscopic study of magnetic behavior of dysprosium doped magnetite nanoparticles. *J. Supercond. Nov. Magn.* **32**(2): 20325–33
[34] Rangasamy V S, Thayumanasundaram S and Locquet J P. 2018. Solvothermal synthesis and electrochemical properties of Na_2CoSiO_4 and Na_2CoSiO_4/carbon nanotube cathode materials for sodium-ion batteries. *Electrochim. Acta* **276**: 102-10
[35] Zhu L, Zeng Y R, Wen J, Li L and Cheng T M. 2018. Structural and electrochemical properties of Na_2FeSiO_4 polymorphs for sodium-ion batteries. *Electrochim. Acta* **292**: 190-8

[36] Nazarkovsky M A, Gun'ko V M, Wójcik G, Czech B, Sobieszek A, Skubiszewska-Zięba J, Janus W and Skwarek E. 2014. Band-gap change and photocatalytic activity of silica/titania composites associated with incorporation of CuO and NiO. *CPTS* **5**(4): 421-37
[37] Świętosławski M, Molenda M, Natkański P, Kuśtrowsk P and Dziembaj R. 2014. Sol–gel synthesis, structural and electrical properties of Li_2CoSiO_4 cathode material. *Funct. Mater. Lett.* **6**(7): 1-4

Acknowledgement
The author would like to thank The University of Lampung for providing financial support for the implementation of this research through research grant with contract numbers 2527/UN26.21/PN/2019.